Optics and Photonics Journal, 2015, 5, 15-27

http://dx.doi.org/10.4236/opj.2015.51003

Nonlinear Change in Refractive Index and Transmission Coefficient of ZnSe:Fe^{2+} at Long-Pulse 2.94-μm Excitation

Alexander V. Kir'yanov[1,2*], Nikolai N. Il'ichev[3], Elmira S. Gulyamova[3], Alexander S. Nasibov[4], Peter V. Shapkin[4]

[1]Centro de Investigaciones en Optica, Loma del Bosque 115, Lomas del Campestre, Leon, Mexico
[2]M.V. Lomonosov Moscow State University, Physics Department, Vorobyevy Gory, 1, Moscow, Russia
[3]A.M. Prokhorov General Physics Institute (Russ. Acad. Sci.), Ul. Vavilova 38, Moscow, Russia
[4]P.N. Lebedev Physical Institute (Russ. Acad. Sci.), Ul. Vavilova 38, Moscow, Russia
Email: *kiryanov@cio.mx

Received 29 December 2014; accepted 16 January 2015; published 20 January 2015

Abstract

An experimental study of the nonlinear changes in refractive index and transmission coefficient of single-crystal ZnSe:Fe^{2+}, fabricated through the Fe-diffusion method, at long-pulse (~300 ns), sub-mJ, 2.94-μm Z-scan probing is reported. As well, a theoretical model based on the generalized Avizonis-Grotbeck equations is developed and applied for straightforward fitting of the open- and closed-aperture Z-scans, obtained for ZnSe:Fe^{2+} with different Fe^{2+} centers concentrations. The modeling results reveal that the contributions in the absorption and refractive index nonlinearities of ZnSe:Fe^{2+} are "common" resonant-absorption saturation (the minor part) and pulse-induced heating of the samples (the major part), which are strongly dependent on Fe^{2+} concentrations. Large values of the index change (>~10^{-3}) and partial resonant-absorption bleaching (limited by ~50%), both produced via the thermal effect mainly, are the features of the ZnSe:Fe^{2+} samples inherent to this type of excitation.

Keywords

Nonlinear Refractive index, Nonlinear Transmission, Z-Scan Technique, Thermal lens, ZnSe:Fe^{2+}

1. Introduction

Single-crystal Fe^{2+}-doped ZnSe is currently the subject of extensive studies since it demonstrates capability of

---

[*] Corresponding author.

How to cite this paper: Kir'yanov, A.V., Il'ichev, N.N., Gulyamova, E.S., Nasibov, A.S. and Shapkin, P.V. (2015) Nonlinear Change in Refractive Index and Transmission Coefficient of ZnSe:Fe^{2+} at Long-Pulse 2.94-μm Excitation. *Optics and Photonics Journal*, **5**, 15-27. http://dx.doi.org/10.4236/opj.2015.51003

being used as an effective laser medium for the spectral region ~4.0 - ~5.0 µm [1]-[11]. The laser property stems from the presence of Fe^{2+} centers, created after doping ZnSe with Fe, which possess of a broad resonant-absorption band spanned from ~2.5 to ~4.5 µm, relevant for pumping by conventional lasers based on Er^{3+}-doped materials [3] [5] [8] [12]-[15]. This band, easily saturated by pulsed radiation, also allows the use of $ZnSe:Fe^{2+}$ as a passive Q-switch cell for ~3-µm Er^{3+}-doped lasers [16]-[18]. Much efforts were made to clarify the physics of $ZnSe:Fe^{2+}$ behind its functioning as a laser or Q-switch element. However certain gaps still exist in the knowledge of some of the featuring $ZnSe:Fe^{2+}$ properties. For instance, the nonlinear-optical characteristics of $ZnSe:Fe^{2+}$ were under scope in a very few works and limited by the studies of resonant-absorption saturation at ~3-µm pumping [16] [19]-[22], with the main result being the estimates for the ground-state absorption (GSA) cross-section σ_{12}. Meanwhile, there is no—as far as we know—any data about the mechanisms and values of nonlinear refractive-index Δn in $ZnSe:Fe^{2+}$ at ~3-µm excitation. The other problem, insufficiently addressed to date is quenching of $ZnSe:Fe^{2+}$ fluorescence, in terms of Fe^{2+} lifetime reduction in regard to temperature and Fe^{2+} concentration, at in-band excitation [1]-[3] [5] [19]-[21].

In the present work, the single-beam Z-scan technique [23] was employed to inspect the nonlinear part of refractive index and nonlinear transmission of $ZnSe:Fe^{2+}$. This technique was successfully applied from the 90-ies for studying versatile nonlinear materials possessing different kinds of amplitude and phase optical nonlinearities. Usually, Z-scan experiments comprise a set of single-beam measurements, allowing determination of the quantities that attribute the nonlinear response of a medium to excitation. The $ZnSe:Fe^{2+}$ samples we deal in the present study have been obtained via the diffusion method, allowing embeding Fe^{2+} centers into the ZnSe matrix in high concentration [20] [24] [25]). In Sections II and III, we study experimentally the nonlinear changes in transmission and refractive index of $ZnSe:Fe^{2+}$ at sub-mJ pulsed 2.94-µm probing by means of the Z-scan technique. [Note that the sole work [19], where the Z-scan technique was applied for $ZnSe:Fe^{2+}$, was targeted at a study of its nonlinear transmission only, not Δn.] In Section IV, we model the problem of propagation of pulsed ~3-µm radiation through $ZnSe:Fe^{2+}$, where the two key nonlinearities are addressed, stemming from saturation of the resonant transition $^5E\rightarrow{}^5T_2$ (Fe^{2+}) and from light-induced heating. In Section V, we discuss the results and reveal the main laws that obey the studied optical nonlinearities, inherent to this type of $ZnSe:Fe^{2+}$ excitation. The conclusions are formulated in Section VI.

2. Experimental Setup and Samples

Setup: The experimental setup is shown in **Figure 1**.

We used as probe the output beam of a flash-lamp pumped actively Q-switched (using an electro-optical $LiNbO_4$ cell) Er^{3+}:YAG laser (1), oscillating in the regime of giant pulses at a wavelength of 2.94 µm. The laser operated at a low repetition rate, 0.5 Hz (a single laser pulse per a flash-lamp shot), ensuring minimal thermal effects in the cavity and, correspondingly, high stability of the output parameters (pulse energy and pulse width). Pulse duration τ_P was fixed (290 ns) in experiments. The laser beam's spatial distribution was made (using an intra-cavity diaphragm,) to be TEM_{00} mode and its polarization was set (by the active element's wedging) almost linear (~1:100). A small portion of the beam was deflected by a CaF_2 plate (2) for monitoring the pulses with a pyro-receiver (3), while its major part was passed in between "folded" Al-reflectors (4) and (5) and focused by a CaF_2 lens (7) (with a focal distance of 30 cm) into a $ZnSe:Fe^{2+}$ sample (8). The beam waist in the focus was measured to be ω_0 = 75 µm. Neutral filters (6) placed in front of the lens allowed varying pulse energy, delivered to the tested sample. Energy of a single pulse, transmitted by the sample, was measured by a pyro-receiver (12), identical to the reference one (3) (note that decay time constants of both the pyro-receivers exceeded 1 ms, which ensured the measured parameter being pulse energy). Open- and closed-aperture Z-scans were obtained by translating the sample along Z-axis around the beam waist, Z_0 (±2.5 cm). When measuring closed-aperture Z-scans, a circular pinhole (9) with a diameter of ~0.6 mm (transmission, ~3%) was placed in front of receiver (12), whereas when measuring open-aperture Z-scans the pinhole was removed from the beam. Neutral filters (10) and a scattering plate (11) were set in front of receiver (12) to avoid its saturation and to homogenize the beam's distribution on the receiver's sensitive head. $ZnSe:Fe^{2+}$ samples were placed on a motorized stage, movable along the laser beam. Each experimental Z-scan point was obtained after averaging over 10 laser pulses, ensuring accuracy of the measurements better than 5%. Signals from the pyro-receivers were recorded using an acquisition board, arranged in the KAMAK's standard, equipped with a PC; the PC also controlled Z-shifting of the stage with a $ZnSe:Fe^{2+}$ sample. In advance to Z-scan experiments, signals from the pyro-receivers have been calibrated by a

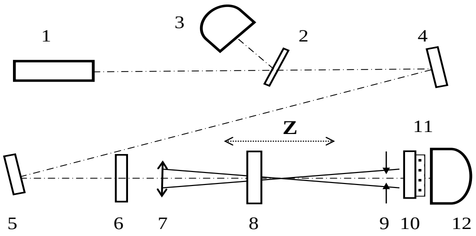

Figure 1. Experimental setup.

calorimeter (placed in the scheme instead of the sample). Pulse energy (E_p) was preserved to be less than 0.58 mJ in the experiments, since at higher pulse energies optical breakdown sporadically happened when ZnSe:Fe^{2+} samples (especially the one with the highest Fe^{2+} concentration) were passed through the focus.

The nonlinear (pulse-energy dependent) changes in ZnSe:Fe^{2+} transmission coefficient and refractive index were determined from the measurements of open- and closed-aperture Z-scans, $T_0(Z)$ and $T_1(Z)/T_0(Z)$ (hereafter Z is the longitudinal coordinate of a sample at its translating along the optical axis). A signal from pyro-receiver (12) in the absence of pinhole (9) gave us, after dividing by input energy (a signal from pyro-receiver (3)), open-aperture Z-scan transmittance. Closed-aperture Z-scan transmittance was obtained by a similar way but with the pinhole placed in front of receiver (12), by means of dividing the measured transmission by the $T_0(Z)$-value. For an absorbing medium (our case), Z-scans $T_0(Z)$ and $T_1(Z)/T_0(Z)$ contain the information about the nonlinear transmission (absorption) and refractive index, respectively. In the present study, we paid most of attention to monitor the nonlinear changes in transmission and in refractive index (Δn) of ZnSe:Fe^{2+} in function of incident pulse energy (E_p).

Samples: Samples of ZnSe:Fe^{2+} were obtained at room temperature through the diffusion process under conditions for the thermodynamic equilibrium of solid ZnSe, solid Fe, and S_{ZnSe}–S_{Fe}–V vapors in evacuated quartz ampules at a He atmosphere; see e.g. Refs. [22] [25]. The diffusion time was variable when getting the ZnSe:Fe^{2+} samples, which gave rise to different average concentrations of Fe^{2+} dopants; see **Table 1**. During the process, opposite sides of pristine single-crystal ZnSe plates with almost parallel faces and thicknesses of ~1.5 mm were subjected to Fe-diffusion. The three studied samples (hereafter samples 464, 422, and 474) were fabricated at the following temperature and diffusion exposure times: 857˚C/241 h (sample 464); 858˚C/216 h (sample 422); 912˚C/192 h (sample 474). After diffusion has been completed, the ZnSe:Fe^{2+} plates were polished at both sides, resulting in ~1-mm thick final samples, with total thicknesses of the areas enriched with Fe^{2+}-centers being 150 - 250 µm. Note that these thicknesses are much less than the confocal parameter's value, z_0~0.6 cm, which validates the "thin sample" approximation [23], used at modeling Z-scans experiments.

The linear ("small-signal") transmission spectra of the samples were recorded using a spectrophotometer; the results are demonstrated in **Figure 2**, for a 500 - 3200-nm region. It is seen that all samples demonstrate a smooth absorption band centered at ~3 µm, characteristic for the Fe^{2+} (transition: $^5E \rightarrow {}^5T_2$) centers. No other features were detected in the spectra, apart an increase of attenuation in the VIS, originated from the ZnSe matrix's band-gap. It is seen that concentrations of Fe^{2+} centers (proportional to extinctions in the ~3-µm band) differ by orders of value in the samples.

3. Experimental Results

In experiments, ZnSe:Fe^{2+} samples were placed almost perpendicularly to the probe beam's propagation. The examples of nonlinear transmittance of samples 464, 422, and 474, measured without a pinhole in front of receiver (12) (*i.e.* open-aperture Z-scans T_0(Z)), and normalized ratio of the nonlinear transmittances, measured with and without the pinhole (*i.e.* closed-aperture Z-scans T_1(Z)), are shown by symbols in **Figure 3(a)-3(c)** and **Figure 3(d)-3(f)**, respectively. In the figure, we demonstrate the data for the maximal pulse energy at the samples incidence (E_p = 0.56 mJ), whereas the data obtained after proceeding similar Z-scans, measured at smaller pulse energies, are collected in **Figure 4(a)-4(b)**. It is seen that substantial transformations in transmissions $T_0(Z)$ and $T_1(Z)$ arise, for all samples, in proximity to the beam waist where the pulse energy density is high. Note that a reference pristine (free from Fe^{2+} doping) ZnSe sample was also under test but no changes in Z-scans $T_0(Z)$ and $T_1(Z)/T_0(Z)$ were found in this case, which ensures an exclusive role of Fe^{2+} centers in the optical nonlinearities induced in ZnSe:Fe^{2+}.

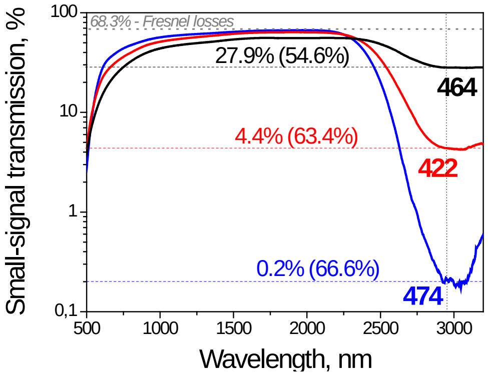

Figure 2. Small-signal transmission spectra of ZnSe:Fe^{2+} with low (sample 464, black curve), intermediate (sample 422, red curve), and high (sample 474, blue curve) Fe^{2+}-centers' concentrations. For each sample, the transmission nearby the resonance (at pump wavelength λ_0 = 2.94 µm) and non-resonant loss, measured far away from the resonant band (in bracket), are provided. The transmission offset stemming from the Fresnel loss at samples' faces is shown by grey line.

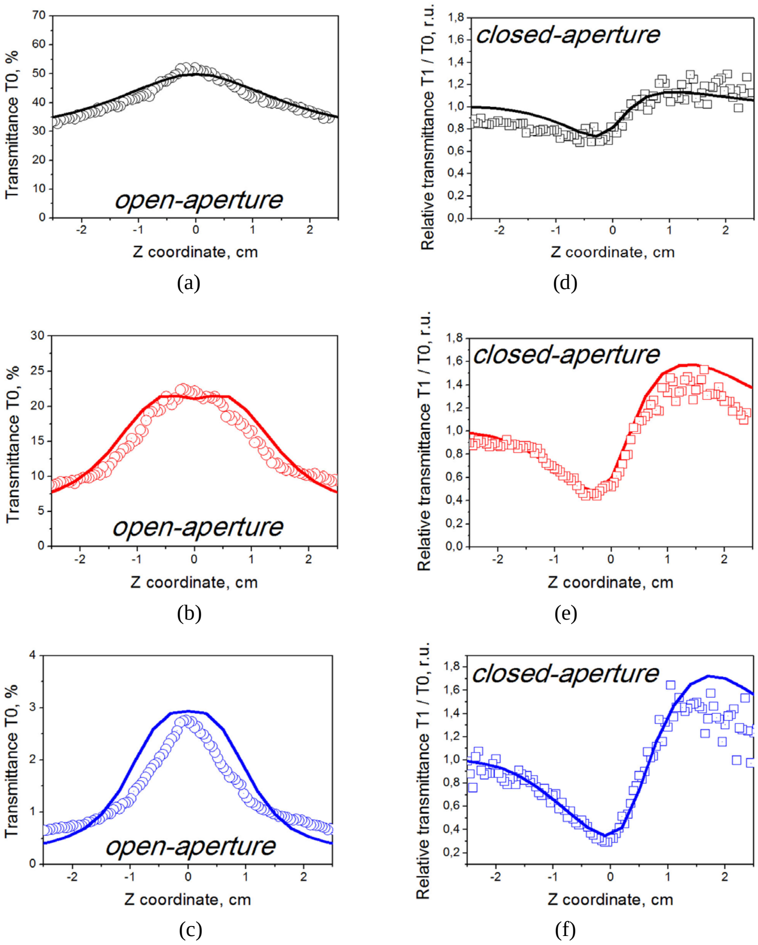

(a) (d)

(b) (e)

(c) (f)

Figure 3. Experimental (empty symbols) and modeled (plain curves) open—(a, b, c) and closed—(d, e, f) aperture Z-scans obtained at pulse energy E_p ~0.56 mJ for ZnSe:Fe^{2+} samples 464 (a, d), 422 (b, e), and 474 (c, f). The whole of the modelled data have been obtained at $\sigma_{12} = 0.86 \times 10^{-18}$ cm^2, ξ = 0.03, and $\eta = -0.4$ and at thicknesses of layers enriched with Fe^{2+} centers being 2l = 140 (sample 464), 170 (sample 422), and 230 (sample 474) µm.

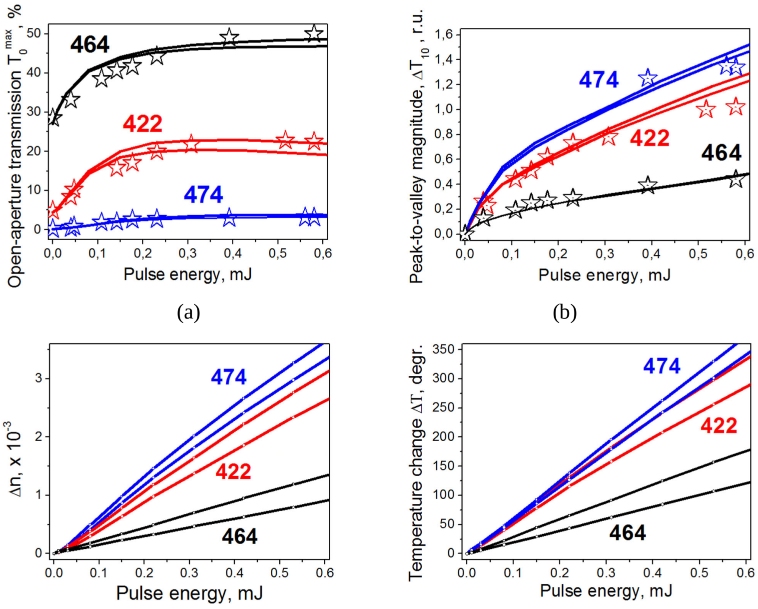

(a) (b)

(c) (d)

Figure 4. (a, b): Maximal transmissions T_0^{max} (a) and peak-to-valley oscillations $T_1/T_0^{max}–T_1/T_0^{max}$ (b), obtained, correspondingly, from open- and closed-aperture Z-scans, for ZnSe:Fe^{2+} samples 464, 422, and 474. The experimental data are shown by empty symbols while the modeling results—by plain fitting curves. (c, d): Dependences of Δ*n*-values (c) and the correspondent temperature changes Δ*T* (d) in samples 464, 422, and 474, obtained as the result of modeling. The whole of the theoretical dependences was obtained at σ_{12} = 0.86 × 10^{-18} cm^2, ξ = 0.04, η = −0.4; thicknesses of the samples' layers enriched with Fe^{2+} were taken as: 2l = 120 and 150 µm (sample 464), 150 and 180 µm (sample 422), and 220 and 260 µm (sample 474).

In case of open-aperture Z-scans (see the left panel in **Figure 3**), rise of T_0 at Z→0 is simply the result of Fe^{2+} centers' resonant-absorption saturation. However an important detail should be noticed, *i.e.* that transmittance $T_0(Z)$—even near the focus—is much less than 100%. This indicates the presence of a source of additional nonlinear loss in the material, the effect explained, as it is demonstrated below, by shortening of Fe^{2+} lifetime via temperature increase under the action of pulsed excitation. Both the phenomena merely contribute in the transmission (absorption) nonlinearity of the samples but the latter contribution dominates at increasing concentration of Fe^{2+} centers: compare graphs (a), (b), and (c) in **Figure 3**.

The closed-aperture transmittances $T_1(Z)/T_0(Z)$ (see the right panel in **Figure 3**), containing the information about the refractive-index nonlinearity in ZnSe:Fe^{2+} samples, also demonstrate drastic perturbations at Z→0. Magnitude of the parameter, characterizing the index nonlinearity, a peak-to-valley "oscillation" between the maximal, T_1/T_0^{max}, and minimal, T_1/T_0^{min}, transmittances, is much bigger (>1.5) for the sample with the highest Fe^{2+} concentration (474, see **Figure 3(f)**) than for the ones with intermediate (422) and the lowest (464) Fe^{2+} concentration (see **Figure 3(e)** and **Figure 3(d)**). The other interesting point is that polarity of Z-scans $T_1(Z)/T_0(Z)$ in all graphs reveals a positive nonlinear lens "created" in the samples. These facts can be only explained by the effect of considerable thermal lensing (an inhomogeneous increase of temperature) in ZnSe:Fe^{2+} at 2.94-µm excitation (the coefficient of thermal dispersion of ZnSe:Fe^{2+} is positive and large [8]).

Figures 4(a)-4(b) (see symbols) reveal the experimental laws that the maximal open-aperture transmittances T_0^{max} and the oscillations $\Delta T_{10} \equiv T_1/T_0^{max} - T_1/T_0^{min}$ in the closed-aperture transmittances obey at varying pulse energy E_p. These data were obtained from the dependences, similar to those presented in **Figure 3** when filters (6) with different attenuations were placed i n front of the samples; refer to **Figure 1**.

These results testify for: 1) that resonant-absorption bleaching (*i.e.* an increase of T_0^{max} with increasing E_p) is incomplete in all samples ($T_0^{max} \ll 100\%$), thus indicating the presence of extra loss induced by pulsed excitation (see **Figure 4(a)**) and 2) that the difference ΔT_{10} (see **Figure 4(b)**), the quantity related to Δ*n*-value, demonstrates a virtually non-saturating behavior with increasing E_p, thus indicating the dominant nonlinearity involved being thermal lensing rather than GSA saturation. The results of modeling, presented in the following section (see "plain" curves fitting the experimental dependences in **Figure 3** and **Figure 4**) confirm these ideas.

4. Modeling

Propagation of a resonant pulse through ZnSe:Fe^{2+}. Propagation of a ~3-μm pulse through a ZnSe:Fe^{2+} sample can be modeled by employing the generalized Avizonis-Grotbeck equations [22] [26]-[28] that describe the interaction of light with a medium with saturable (resonant) absorption. However this model requires certain modifications in order to address: 1) the effect of heating of a ZnSe:Fe^{2+} sample by a pulse since an increase of temperature during excitation should ought to shorten Fe^{2+} lifetime (as the result, Fe^{2+} lifetime cannot be fixed at modeling but rather should be a parameter, dependent on pulse energy, accumulated and dissipated in the sample, and therefore on temperature's growth; 2) the effect of experiencing by a pulse of "extra" loss in ZnSe:Fe^{2+}, an "alter-ego" for incomplete resonant-absorption bleaching of ZnSe:Fe^{2+} (which stems from the mentioned pulse-induced Fe^{2+} lifetime reduction); 3) the thermal-lens effect, thereby contributing in overall refractive-index nonlinearity.

Basic equations: To describe propagation of a pulse at a wavelength resonant to ZnSe:Fe^{2+} transition $^5E\rightarrow^5T_2$ at arbitrary ratio of the pulse duration to the Fe^{2+} centers upper level's relaxation time, we employed the following equations:

$$\frac{\mathrm{d}n_2}{\mathrm{d}t} = -\sigma_{21} n_2 I + \sigma_{12} n_1 I - \frac{n_2}{\tau_r(T)} \tag{1a}$$

$$\frac{\mathrm{d}I}{\mathrm{d}z} = -\sigma_{12} n_1 I + \sigma_{21} n_2 I - \gamma I \tag{1b}$$

We consider here a two-level scheme for Fe^{2+} centers with lower 1 (^{5}E) and upper 2 ($^5T_2$) levels, in accordance to the model of ZnSe:Fe^{2+} energy states; see e.g. Refs. [2] [5]. In this system of equations, n_1 and n_2 are the population densities of levels 1 and 2, respectively; $\tau_r(T)$ is the lifetime of the upper level, which depends on ZnSe:Fe^{2+} temperature T (see below); σ_{12} and σ_{21} are the cross-sections of absorption from level 1 to level 2 and stimulated emission from level 2 to level 1, respectively, for a given wavelength λ_0 within the Fe^{2+}-centers' GSA-contour (considered to be homogeneously-broaden); I is the pulse intensity in photons/(cm^2·s); and z is the coordinate running through ZnSe:Fe^{2+} (it should be not confused with Z-coordinate of a sample positioned as the whole with respect to the beam waist). In system (1a, 1b), the first equation describes the variation in populations of levels 1 and 2 with time and the second one—the variation in pulse intensity upon propagation in the sample. It is implicitly implied that $n_1 + n_2 = n_0$, *i.e.* that the sum of Fe^{2+} centers' populations of levels 1 and 2 is equal to overall concentration of Fe^{2+} centers n_0, which holds at the absence of photo-induced processes (probably leading to variations in valence).

Following the approach [27], the equation for phase difference $\Delta\varphi_{sat}$, experienced by phase φ of the pulse travelling in the sample (which is complementary to the resonant-absorption saturation process addressed by Equation (1) via Kramers-Kronig relations), can be written as:

$$\frac{\mathrm{d}(\Delta\varphi_{sat})}{\mathrm{d}z} = \frac{\alpha_0 \delta}{2}\left(\frac{n_1}{n_0} + \eta\frac{n_2}{n_0}\right) \tag{2}$$

where α_0 is the small-signal absorption (GSA) of ZnSe:Fe^{2+} and δ and η are the coefficients that concern to the relations between the real (χ') and imaginary (χ'') parts of ZnSe:Fe^{2+} susceptibilities in the ground (1) and excited (2) states at λ_0. Parameters δ and η are defined as follows:

$$\delta = \frac{\chi_1'}{\chi_1''} \tag{3a}$$

$$\eta = \frac{\chi_2'}{\chi_1'} \tag{3b}$$

and can be found similarly to [27] [28] as Fe^{2+} absorption and fluorescence spectra are well-known for ZnSe:Fe^{2+}; see e.g. Refs. [1]-[3] [5] [8] [11] [18] [20] [21]. Equations (1)-(2) hold at rather weak assumptions that pulse duration τ_P is significantly bigger than passing time through the sample and that excited-state absorption (ESA) from state 2 to the above lying states is null.

For the case of a rectangular pulse with duration τ_P, system of Equations (1)-(2) is reduced to the equation that addresses variation in the pulse energy density $\varepsilon = I_0\tau_P(\sigma_{12}+\sigma_{21})$ (in photons):

$$\frac{\mathrm{d}\varepsilon}{\mathrm{dz}} = -\alpha_0\frac{\varepsilon\xi}{1+\varepsilon\xi}\left(\frac{1}{\xi}+S(\varepsilon)\right)-\gamma\varepsilon \tag{4}$$

and to the equation for ε-dependent phase difference $\Delta\varphi_{\mathrm{sat}}$:

$$\frac{\mathrm{d}(\Delta\varphi_{sat})}{\mathrm{dz}} = \frac{\alpha_0\delta}{2}\left(1-\frac{\sigma_{12}}{\sigma_{12}+\sigma_{21}}S(\varepsilon)(1-\eta)\right) \tag{5}$$

where $n_2(\varepsilon)=\alpha_0 S(\varepsilon)/(\sigma_{12}+\sigma_{21})$ and $n_1(\varepsilon)=\alpha_0/\sigma_{12}-n_2(\varepsilon)$ and function $S(\varepsilon)$ and ratio of Fe^{2+} lifetime to pulse duration, $\xi(T)$, are written as $S(\varepsilon)=\varepsilon\xi\left(1-\exp\left(-\varepsilon-\frac{1}{\xi}\right)\right)\Big/(1+\varepsilon\xi)$ and $\xi(T)=\tau_r(T)/\tau_P$, respectively. Note that at $\xi(T)\ll 1$ and $\xi(T)\gg 1$, Eq. (2) transforms to the "standard" Avizonis-Grotbeck equation [26]:

$$\frac{\mathrm{d}\varepsilon}{\mathrm{dz}} = -\alpha_0\left(1-\exp(-\varepsilon)\right)-\gamma\varepsilon \tag{6a}$$

and to the well-known equation (for intensities):

$$\frac{\mathrm{d}I_0}{\mathrm{dz}} = -\alpha_0\frac{I_0}{1+I_0/I_s}-\gamma I_0, \tag{6b}$$

where $I_s=\left[\tau_r(T)(\sigma_{12}+\sigma_{21})\right]^{-1}$ is the saturating intensity.

System of Equations (4)-(5) can be used for modeling of a pulse's propagation through a medium with a single resonance (for an arbitrary $\xi(T)$-value). Specifically, Equation (4) addresses the interaction of pulsed radiation with the medium (and allows one to calculate the nonlinear change in transmission $T_0(\varepsilon)$), whilst Equation (5) addresses the phase change (and allows one to determine the nonlinear change in refractive index, $\Delta n_{sat}(\varepsilon)$).

Temperature impact: Furthermore, attention should be paid to an important issue (regarding ZnSe:Fe^{2+}), the mentioned strong dependence of lifetime of excited Fe^{2+} centers upon temperature. Apparently, the higher SSA α_0 of ZnSe:Fe^{2+} and the bigger pulse energy E_P, the higher an increase of temperature $\Delta T \sim \alpha_0 E_P$ in the crystal (at neglecting thermal diffusion). As simple estimates show, heating of ZnSe:Fe^{2+} samples by 2.94-µm pulses can be, in our experiments, of the order of hundreds degrees. Thus, statements (i) and (ii) made above ought to be addressed by means of incorporating the dependence $\tau_r(T)$ into the model.

There are evidences to consider shortening of Fe^{2+} centers lifetime, or "fluorescence temperature quenching", to originate from strong electron-phonon coupling [3] [5] [21]. This phenomenon can be addressed by the following law:

$$\frac{1}{\tau_r(T)} = \frac{1}{\tau_{rad}}+W_0\exp\left(-\frac{\Delta E_a}{k_B T}\right), \tag{7}$$

where τ_{rad} is the radiative lifetime of Fe^{2+} centers, W_0 is the parameter that stands for non-radiative relaxation (on ZnSe phonons), ΔE_a is the activation energy, and k_B is Boltzmann constant. The best fit of the known data for $\tau_r(T)$ [1]-[3] [5] [21] [29] (see asterisks in **Figure 5**) is obtained at the parameters' values: ΔE_a = 1750 cm^{-1}, $1/W_0$ = 0.1 ns, and τ_{rad} = 350 ns (at room temperature); see the plain curve in the figure.

Since both Equations (4)-(5) contain the terms dependent upon $\tau_r(T)$ (in fact, upon $\xi(T)=\tau_r(T)/\tau_P$), an account of the temperature quenching effect in ZnSe:Fe^{2+} (7) becomes a necessary modeling's chain. Furthermore, heating of ZnSe:Fe^{2+} by radiation, resonant to the Fe^{2+} GSA band, should also contribute in its refractive index nonlinearity. If a ~3-µm pulse propagates through ZnSe:Fe^{2+}, not only the "resonant" contribution in refractive index $\Delta n_{sat}(\varepsilon)$ (associated with perturbations of Fe^{2+} energy levels—see Equation (4) (5)) arises, but also the "thermal" one $\Delta n_{th}(\varepsilon)$ (stemmed from inhomogeneous heating of the sample). Assuming that for a ~300-ns pulse (our case) thermal diffusion in ZnSe:Fe^{2+} is negligible, the equation addressing the thermal effect can be written as:

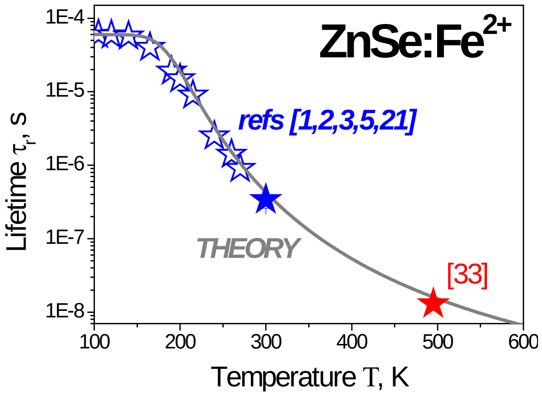

Figure 5. Temperature dependence of Fe^{2+} centers' lifetime τ_r. The asterisks of different colors correspond to the experimental results [1]-[3] [5] [21] [29] and the plain curve (labeled "theory") is the fit made using Formula (7).

$$\frac{\mathrm{d}\left(\Delta\varphi_{th}\right)}{\mathrm{d}z} = k_0 \frac{\mathrm{d}n}{n\mathrm{d}T}\frac{\alpha_0 h\varepsilon}{\rho C}, \tag{8}$$

where n, $\mathrm{d}n/\mathrm{d}T$, ρ, and C are the refractive index, thermal dispersion, density, and specific heat of ZnSe:Fe^{2+}, respectively, and $k_0 = 2\pi/\lambda_0$. By writing Formula (8), we implicitly assume that the pulse energy is entirely dissipated on ZnSe phonons, given that Stokes loss is ≈100% because the excitation part, leaving a ZnSe:Fe^{2+} sample in the form of Fe^{2+} fluorescence, is tiny (<1% [8]). Note that Equation (8) was obtained at the same assumption of a square-shape intensity distribution inside the sample, made when deriving Equations (4)-(5). The other assumption, about negligible thermal diffusion, is proven by insignificant temperature re-distribution in ZnSe:Fe^{2+} during the pulse action, given by very low thermal diffusivity of ZnSe ($D_{th} = \Lambda/\rho C = 0.1\ \mathrm{cm}^2\cdot\mathrm{s}^{-1}$, where ρ = 5.26 g·cm^{-3}, C = 0.34 J·g^{-1}·K^{-1}, and Λ = 0.19 W·cm^{-1}·K^{-1} are density, specific heat, and thermal conductivity, respectively). An estimate for the heat's diffusion length at τ_P~300 ns (our case) is ~2 μm, which is much less than the spatial area where heat is generated, in turn estimated by the Z-scan beam radius $\omega(Z)$ at the sample's location (even at the focus it is measured by ω_0 =75 μm).

The overall phase change, experienced by a pulse, passing through ZnSe:Fe^{2+}, is the sum of the changes, "generated" by the GSA saturation and thermal effects (see Equation (5) and Equation (8)):

$$\frac{\mathrm{d}\left(\Delta\varphi_{\text{total}}\right)}{\mathrm{d}z} = \frac{\mathrm{d}\left(\Delta\varphi_{sat}\right)}{\mathrm{d}z} + \frac{\mathrm{d}\left(\Delta\varphi_{th}\right)}{\mathrm{d}z} \tag{9}$$

Z-scan formalism: At making numerical calculations, we assumed that the Z-scan beam is spatially Gaussian, *i.e.* that the following conditions at the sample's entrance hold:

$$\varepsilon^0 = \frac{2\varepsilon_{in}}{\pi\omega^2}\exp\left(-\frac{2r^2}{\omega^2}\right);\ \varphi^0 = Z + k_0\frac{r^2}{2R} \tag{10}$$

where r is the radius of the Gaussian envelope, $\omega(Z)$ and $R(Z) = Z + Z_0^2/Z$ are, respectively, the spot-size and radius of the beam curvature, Z is the sample's position with respect to the beam waist [Z_0 = 0, $R_0 \equiv R(Z_0 = 0) = \infty$ and $\omega_0 \equiv \omega(Z_0 = 0)$], and $z_0 = \pi\omega_0^2/\lambda_0$ is the confocal parameter. The calculations were performed for each Z, designating the sample's position as the whole with respect to the focus. As the result of calculating Equations (4) (5) (8), the output pulse energy and phase (ε^{out} ($z = L$) and φ^{out} ($z = L$)) were obtained and, consequently, the open- and closed-aperture transmissions:

$$T_0(Z) = \frac{\int_0^\infty \varepsilon^{\text{out}} r\mathrm{d}r}{\int_0^\infty \varepsilon^0 r\mathrm{d}r} \tag{11}$$

$$\frac{T_1(Z)}{T_0(Z)}=\frac{\mathrm{E}(Z)\mathrm{E}^*(Z)}{\mathrm{E}(0)\mathrm{E}^*(0)} \tag{12}$$

where Kirchhoff integral is taken over a pinhole transmitting a small part of pulse energy $\mathrm{E}(Z)=ik_0\int_0^\infty \mathrm{E}^{\mathrm{out}}\,2\pi r\mathrm{d}r\big/(d-Z)$, with d being the distance between the pinhole and focal point $\left(\mathrm{E}^{\mathrm{out}}(Z)\propto\sqrt{\varepsilon^{\mathrm{out}}}\,\mathrm{e}^{-i\left(\frac{k_0r^2}{2R}+\frac{k_0r^2}{2(d-Z)}+\Delta\varphi\right)}\right)$. The total phase difference and change in refractive index of ZnSe:Fe^{2+} were found as:

$$\Delta\varphi(Z)=\frac{\int_0^\infty\left(\varphi^{\mathrm{out}}-\varphi^0\right)\varepsilon^0 r\mathrm{d}r}{\int_0^\infty \varepsilon^0 r\mathrm{d}r}, \tag{13}$$

$$\Delta n(Z)=\frac{\Delta\varphi(Z)}{k_0 n L_{eff}}\approx\frac{\alpha_0\Delta\varphi(Z)}{k_0 n\left(1-\exp(-\alpha_0 L)\right)}, \tag{14}$$

where L_{eff} is the effective thickness [30] of the sample.

Parameters' values employed at modeling: Thickness of two opposite layers enriched with Fe^{2+}, $L = 2l$ (l is the thickness of a single layer), was estimated for each sample using the method [25]. It was found that L is measured from ~150 µm (sample 464) to ~250 µm (sample 474), depending on the doping temperature, Fe^{2+} diffusion time, and polishing conditions. Therefore L was varied in the modeling around these values (see e.g. **Figure 4(a)** and **Figure 4(b)**). Accordingly, the average Fe^{2+} concentrations n_0, SSA-values α_0, and passive losses γ were determined; see **Table 1**. The saturation energy density was fixed in calculations (E_s =0.08 J/cm^2) as defined by the value of the GSA cross-section $\sigma_{12}=0.86\times10^{-18}\ \mathrm{cm}^2$ (at λ_0 = 2.94 µm), while the stimulated-emission cross-section was zeroed (σ_{12} = 0). The values of parameters δ and η, characterizing the relations between the real and imaginary susceptibilities of ZnSe:Fe^{2+}, were found from the absorption and fluorescence spectra of Fe^{2+} centers [1]-[3] [5] [8] [11] [18] [20] [21] in analogy to [27] [28]. The most reliable values of these parameters were found to be δ = 0.03 and η = −0.4 (at λ_0 = 2.94 µm). Pulse duration at the samples' incidence was fixed: τ_P =290 ns. To address the thermal effect in ZnSe:Fe^{2+}, the following quantities were taken: n = 2.43 and $\mathrm{d}n/\mathrm{d}T=7\times10^{-5}$ [8]. The temperature dependence of Fe^{2+} lifetime τ_r was accounted for by means of Formula (7).

5. Discussion

The results of modeling (see plain curves in **Figure 3** and **Figure 4**) are seen to fit well the whole of the experimental data (see symbols in the figures). Importantly, this agreement has been reached for all samples 464, 422, and 474 without varying neither the GSA cross-section σ_{12}, nor the parameters δ and η.

Transmission (absorption) nonlinearity: First, the strongly limited absorption "bleaching" (*i.e.* the strongly reduced transmission T_0) at high pulse energies (see **Figure 3(a)-Figure 3(c)** and **Figure 4(a)**) and almost unsaturated magnitude of T_1/T_0-oscillation, proportional to Δn (see **Figure 3(d)-Figure 3(f)** and **Figure 4(b)**), should be noticed. This testifies for the reason explaining these features being "pulse-induced loss", which can be solely related to a strong increase of temperature of ZnSe:Fe^{2+} samples under the pulse action (through the temperature-induced Fe^{2+} fluorescence quenching phenomenon; refer to **Figure 5**). Furthermore, since an account of the thermal effect is one of the key points in the model, a dependence of temperature change ΔT in ZnSe:Fe^{2+} upon pulse energy $\mathrm{E_P}$ is easily obtainable. Such dependences for samples 464, 422, and 474 are demonstrated in **Figure 4(d)**. They, expectedly almost linear on pulse energy for either sample, reveal rise of temperature up to hundreds degrees over room temperature. This allows understanding of the crucial role of Fe^{2+} lifetime reduction at increasing T; refer to (7).

Figure 6 demonstrates an illustration of what happens with the absorptive properties of ZnSe:Fe^{2+} in terms of optical density OD = –ln(T_0) and pulse-induced loss, both normalized on the values of initial optical density OD$_0$ = $\alpha_0 L$ (see **Table 1**), vs. pulse energy $\mathrm{E_P}$. The OD-values in **Figure 6** were obtained after re-calculating the data

Table 1. Samples' parameters.

#	Optical density OD_0	Doped layers thickness 2l, μm	*Samllsignal absorption α_0, cm^{-1}	*passive loss γ, cm^{-1}	*Fe^{2+} average concentration n_0, cm^{-3}
464	1.3	135 ± 15	51	43	0.6×10^{20}
422	3.1	165 ± 15	157	27	1.9×10^{20}
474	6.2	240 ± 20	242	17	2.8×10^{20}

*Defined with accuracy given by the estimates for the samples' thicknesses.

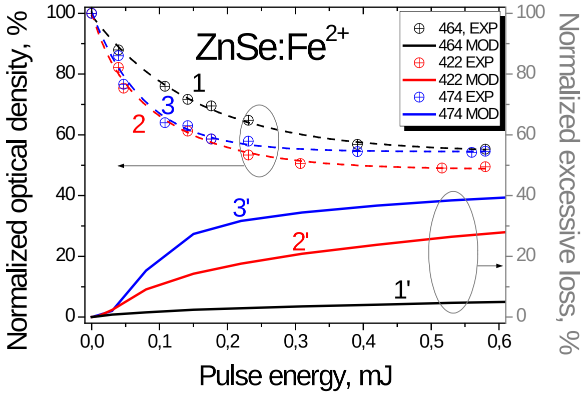

Figure 6. Dependences of normalized optical densities (curves 1, 2, and 3) and normalized excessive losses (curves 1', 2', and 3') upon pulse energy for samples 464 (curves 1 and 1'), 422 (curves 2 and 2'), and 474 (curves 3 and 3'). Crossed points are the experimental data (see **Figure 4(a)** and **Table 1**) and dashed lines are the fits (plain curves are the modeling results).

presented in **Figure 4(a)**, whereas the values of pulse-induced loss (obtained from modeling made with and without an account of Fe^{2+} lifetime reduction). [Note that all dependences shown in **Figure 6** were obtained for ZnSe:Fe^{2+} samples placed at the probe beam's focus, $Z_0 = 0$.]

It is seen that the normalized optical densities of the samples (see curves 1, 2, and 3), though decreasing at increasing pulse energy, do not approach zero, being instead limited by ~50%. Furthermore, the higher Fe^{2+} concentration in ZnSe:Fe^{2+}, the steeper is a decrease of OD vs. E_P. In turn, the normalized excessive losses in the samples (see curves 1', 2', and 3') largely increase at increasing pulse energy; moreover, the higher Fe^{2+} concentration, the higher is the loss magnitude (say, at E_P ~0.56 mJ the pulse-induced losses in samples 464 and 474 are measured by ~5% and ~40%, respectively). Presumably, these trends are an appearance of temperature-induced Fe^{2+} fluorescence quenching. To the best of our knowledge, the revealed laws were never reported for ZnSe:Fe^{2+}.

Refractive index nonlinearity: *One* more point deserving attention is the dependence of refractive-index nonlinearity Δn on pulse energy E_P (see **Figure 4(c)**), which was obtained after modeling the closed-aperture Z-scans, presented in **Figure 3(d)-Figure 3(f)**. When compared with the dependence $\Delta T(E_P)$ (**Figure 4(d)**), the behavior of Δn vs. E_P becomes clear as mostly stemming from a temperature rise. Indeed, the thermal nonlinearity Δn_{th} is seen to dominate in ZnSe:Fe^{2+} index change. On the other hand, the "resonant" part Δn_{sat}, associated with the GSA saturation (via Kramers-Kronig relations), was found—when it was calculated separately—to saturate with increasing E_P. However, magnitude of this contribution is $<5 \times 10^{-5}$, *i.e.* Δn_{sat} is always much less than Δn_{th} ($>10^{-3}$ at the highest pulse energy).

The approach limitations: In spite of satisfactory agreement between the experimental data and theory, certain imperfections can be noticed in details: e.g. it is seen that with increasing Fe^{2+} concentration (in a sequence of samples 464→422→474), the shapes of the modelled Z-scans get deviated from the experimental ones; **Figure 3(a)-Figure 3(c)**. Certain uncertainties can be also noticed in the behavior $T_0(E_P)$; **Figure 4(a)**.

A possible cause that stands behind the imperfection of the modeling is the assumption about homogeneity of Fe^{2+} distribution within the doped layers, which is no more than a rough approximation: in reality, Fe^{2+} concentration profiles in ZnSe:Fe^{2+} fabricated by the diffusion method (our case) satisfy the errors' function [25]. Another problem seems to be the lack of account of such effects as "concentration-related Fe^{2+} fluorescence quenching" [20] [21] [31] and, hypothetically, a photo-induced process at ~3-µm excitation [15] [32] [33], which would lead to valence variation in ZnSe:Fe^{2+}. One more factor responsible for the mentioned deviations can be depression of the Fe^{2+} GSA-band at elevated temperatures (at high-energy excitation). This effect results in a fall of the GSA cross-section σ_{12} near λ_0 =3 µm (see e.g. Ref. [29]). [Notice that an estimate for Fe^{2+} lifetime in ZnSe at high temperatures (<12 ns at T = 220˚C) [33]), fits well the dependence plotted in **Figure 5** (see the red asterisk).]

It should be also emphasized that our model apparently disregards the known fact that at high temperatures (above 200˚C - 250˚C) ZnSe is chemically unstable and oxidizes into ZnO. The model's prediction concerning an increase of temperature, established in ZnSe:Fe^{2+} under the pulse action, tells that T can be as high as 300˚C - 350˚C; however, this happens for the highest E_P (>0.55 mJ) and only for the sample with the highest Fe^{2+} content (474) and exactly at the bean focus; refer to **Figure 4(d)**. Probably, the mentioned chemical instability of ZnSe:Fe^{2+} at largely elevated T led to sporadic optical breakdown, happened near the focus at these conditions (see Section II). The absence or vanishing probability of optical breakdown in the samples with lower Fe^{2+} contents (422 and 464) is seemingly a demonstration that the highest temperatures induced in them (refer again to **Figure 4(d)**) never reach the "critical" ones, at which the chemical instabilities and a trend to oxidizing become notable in ZnSe.

Usefulness for future studies: We believe that, given by increasing interest to ZnSe:Fe^{2+} as to a perspective laser material for the spectral range ~4.5 - 5 µm (see e.g. reviews [34] [35]), the issues highlighted in this work are worth of attention. In particular, capacity of effective lasing that the use of ZnSe:Fe^{2+} samples fabricated through the Fe-diffusion method [6] [36] provides (like the ones inspected above), ensures relevance and usefulness of the current study.

6. Conclusion

We reported a study of the energy-dependent nonlinear transmission coefficient and nonlinear change in refractive index of mono-crystalline ZnSe:Fe^{2+}, fabricated by the diffusion method, at pulsed 2.94-µm Z-scanning. The experiments were fulfilled with a set of ZnSe:Fe^{2+} samples with different Fe^{2+} concentrations, at variable energy of a probe pulse and fixed pulse duration (290 ns). The following basic trends were found to exist. First, a dominant role of the pulse-induced thermal effect is established in the transmission/refractive-index nonlinearities of ZnSe:Fe^{2+} while there is little impact of the resonant-absorption saturation. Second, the thermal effect itself is manifested through: 1) Fe^{2+} lifetime reduction (temperature quenching) and 2) thermal lensing, with both phenomena associated to significant growth of ZnSe:Fe^{2+} temperature under the pulse action. The large values of refractive-index nonlinearity (of the order of 10^{-3}), partial resonant-absorption bleaching (not exceeding ~50%), and pulse-induced excessive loss (measured by tens of percent of the initial optical density of the samples) at maximal pulse energy (~0.55 mJ) are the main features revealed for this type of ZnSe:Fe^{2+} crystals.

Acknowledgements

This work was supported by the Russian Fund for Basics Research (Russia) through the Projects 13-02-01073a, 12-02-00641a, 12-02-00465a, and 13-02-12181 ofi-m, by the grant of President of Russian Federation for state support of the leading scientific schools of Russian Federation NSh-451-2014.2.

References

[1] Adams, J.J., Bibeau, C., Page, R.H., Krol, D.M., Furu, L.H. and Payne, S.A. (1999) 4.0-4.5-µm Lasing of Fe:ZnSe below 180 K, a New Mid-Infrared Laser Material. *Optics Letters*, **24**, 1720-1722. http://dx.doi.org/10.1364/OL.24.001720

[2] Kernal, J., Fedorov, V.V., Gallian, A., Mirov, S.B. and Badikov, D.V. (2005) 3.9-4.8 µm Gain-Switched Lasing of Fe:ZnSe at Room Temperature. *Optics Express*, **13**, 10608-10615. http://dx.doi.org/10.1364/OPEX.13.010608

[3] Kernal, J., Fedorov, V.V., Gallian, A., Mirov, S.B. and Badikov, D.V. (2006) 3.9-4.8 µm Gain-Switched Lasing of Fe:ZnSe at Room Temperature. In: Hoffman, H.J. and Shori, R.K., Eds., *Solid State Lasers XV*: *Technology and Devices*, *Proceedings of SPIE*, Vol. 6100, 61000F.

[4] Akimov, V.I., Voronov, A.A., Kozlovsky, V.I., Korostelin, Yu.V., Landman, A.I., Podmar'kov, Yu.P. and Frolov, M.P. (2006) Efficient Lasing in Fe^{2+}:ZnSe Crystal at Room Temperature. *Quantum Electronics*, **36**, 299-301. http://dx.doi.org/10.1070/QE2006v036n04ABEH013139

[5] Fedorov, V.V., Mirov, S.B., Gallian, A., Badikov, D.V., Frolov, M.P., Korostelin, Y.V., Kozlovsky, V.I., Landman,

A.I., Podmar'kov, Y.P., Akimov, V.A. and Voronov, A.A. (2006) 3.77-5.05 µm Tunable Solid-State Lasers Based on Fe^{2+}-Doped ZnSe Crystals Operating at Law and Room Temperatures. *IEEE Journal of Quantum Electronics*, **42**, 907-917. http://dx.doi.org/10.1109/JQE.2006.880119

[6] Il'ichev, N.N., Danilov, V.P., Kalinushkin, V.P., Studenikin, M.I., Shapkin, P.V. and Nasibov, A.S. (2008) Superluminescent Room-Temperature Fe^{2+}:ZnSe IR Radiation Source. *Quantum Electronics*, **38**, 95-96. http://dx.doi.org/10.1070/QE2008v038n02ABEH013786

[7] Doroshenko, M.E., Basiev, T.T., Koranda, P., Jelinkova, H., Nemec, M., Cech, M., Sulc, J., Komar, V.K., Gerasimenko, A.S., Badikov, V.V. and Badikov, D.V. (2009) Bulk Fe:ZnSe Laser Gain-Switched by the Q-Switched Er:YAG Laser. In: Clarkson, A., Hodgson, N. and Shori, R.K., Eds., *Solid State Lasers XVIII*: *Technology and Devices*, *Proceedings of SPIE*, Vol. 7193, 71931K.

[8] Mirov, S., Fedorov, V., Moskalev, I., Martyshkin, D. and Kim, C. (2010) Progress in Cr and Fe Doped Mid-IR Laser Materials. *Laser and Photonics Review*, **4**, 21-41. http://dx.doi.org/10.1002/lpor.200810076

[9] Doroshenko, M.E., Jelınkova, H., Koranda, P., Sulc, J., Basiev, T.T., Osiko, V.V., Komar, V.K., Gerasimenko, A.S., Puzikov, V.M., Badikov, V.V. and Badikov, D.V. (2010) Tunable Mid-Infrared Laser Properties of Cr^{2+}:ZnMgSe and Fe^{2+}:ZnSe Crystals. *Laser Physics Letters*, **7**, 38-45. http://dx.doi.org/10.1002/lapl.200910111

[10] Myoung, N.S., Martyshkin, D., Fedorov, V.V., Martinez, A. and Mirov, S.B. (2011) Energy Scaling of Room Temperature Fe^{2+}:ZnSe Gain-Switched 4.3 µm Laser. In: Clarkson, A., Hodgson, N. and Shori, R.K., Eds., *Solid State Lasers XX*: *Technology and Devices*, *Proceedings of SPIE*, Vol. 7912, 79121C.

[11] Doroshenko, M.E., Jelinkova, H., Basiev, T.T., Jelinek, M., Koranda, P., Nemec, M., Komar, V.K., Gerasimenko, A.S., Badikov, V.V., Badikov, D.V., Vyhlidal, D. and Stoklasa, J. (2011) Fe:ZnSe Laser—Comparison of Active Materials Grown by Two Different Methods. In: Clarkson, A., Hodgson, N. and Shori, R.K., Eds., *Solid State Lasers XX*: *Technology and Devices*, *Proceedings of SPIE*, Vol. 7912, 79122D.

[12] DeLoach, L.D., Page, R.H., Wilke, G.D., Payne, S.A. and Krupke, W.F. (1996) Transition Metal-Doped Zinc Chalcogenides: Spectroscopy and Laser Demonstration of a New Class of Gain Media. *IEEE Journal of Quantum Electronics*, **32**, 885-895. http://dx.doi.org/10.1109/3.502365

[13] Page, R.H., Schaffers, K.I., DeLoach, L.D., Wilke, G.D., Patel, E.D., Tassano, J.B., Payne, S.A., Krupke, W.F., Chen, K.T. and Burger, A. (1997) Cr^{2+}-Doped Zinc Chalcogenides as Efficient, Widely Tunable Mid-Infrared Lasers. *IEEE Journal of Quantum Electronics*, **33**, 609-619. http://dx.doi.org/10.1109/3.563390

[14] Brik, M.G. (2007) Comparative First-Principles Analysis of Crystal Field Splitting, Charge Transfer Energies and Covalent Effects for Cr^{2+} and Fe^{2+} Ions in II-VI and III-V Compounds. *Journal of Materials Science*: *Materials in Electronics*, **18**, 221-224. http://dx.doi.org/10.1007/s10854-007-9199-3

[15] Kalyuk, L.L., Laiho, R., Lashkul, A.V., Lahderanta, E., Nedeoglo, D.D., Nedeoglo, N.D., Radevici, I.V., Siminel, A.V., Sirkeli, V.P. and Sushkevich, K.D. (2010) Magnetic and Luminescent Properties of Iron-Doped ZnSe Crystals. *Physica B*, **405**, 4330-4334. http://dx.doi.org/10.1016/j.physb.2010.07.036

[16] Kisel, V.E., Shcherbitskii, V.G., Kuleshov, N.V., Postnova, L.I. and Levchenko, V.I. (2005) Saturable Absorbers for Passive Q-Switching of Erbium Lasers Emitting in the Region of 3 µm. *Journal of Applied Spectroscopy*, **72**, 818-823. http://dx.doi.org/10.1007/s10812-006-0009-0

[17] Voronov, A.A., Kozlovsky, V.I., Korostelin, Yu.V., Landman, A.I., Podmar'kov, Yu.P., Polushkin, V.G. and Frolov, M.P. (2006) Passive Fe^{2+}:ZnSe Single-Crystal Q Switch for 3-µm Lasers. *Quantum Electronics*, **36**, 1-2. http://dx.doi.org/10.1070/QE2006v036n01ABEH013097

[18] Gallian, A., Martinez, A., Marine, P., Fedorov, V., Mirov, S., Badikov, V., Boutoussov, D. and Andriasyan, M. (2007) Fe:ZnSe Passive Q-Switching of 2.8-µm Er:Cr:YSGG Laser Cavity. In: Hoffman, H.J., Shori, R.K. and Hodgson, N., Eds., *Solid State Lasers XVI*: *Technology and Devices*, *Proceedings of SPIE*, Vol. 6451, 64510L.

[19] Cankaya, H., Demirbas, U., Erdamar, A.K. and Sennaroglu, A. (2008) Absorption Saturation Analysis of Cr^{2+}:ZnSe and Fe^{2+}:ZnSe. *Journal of the Optical Society of America B*, **25**, 794-800. http://dx.doi.org/10.1364/JOSAB.25.000794

[20] Myoung, N.S., Fedorov, V.V. and Mirov, S.B. (2010) Opticaly Dense Fe:ZnSe Crystals for Energy Scaled Gain Switched Lasing. In: Clarkson, A., Hodgson, N. and Shori, R.K., Eds., *Solid State Lasers XIX*: *Technology and Devices*, *Proceedings of SPIE*, Vol. 7578, 75781H.

[21] Myoung, N.S., Fedorov, V.V., Mirov, S.B. and Wenger, L.E. (2012) Temperature and Concentration Quenching of Mid-IR Photoluminescence in Iron Doped ZnSe and ZnS Laser Crystals. *Journal of Luminescence*, **132**, 600-606. http://dx.doi.org/10.1016/j.jlumin.2011.10.009

[22] Il'ichev, N.N., Shapkin, P.V., Kulevsky, L.A., Gulyamova, E.S. and Nasibov, A.S. (2007) Nonlinear Transmittance of ZnSe:Fe^{2+} at a Wavelength of 2.92 µm. *Laser Physics*, **17**, 130-133. http://dx.doi.org/10.1134/S1054660X07020132

[23] Sheik-Bahae, M., Said, A.A., Wei, T., Hagan, D.J. and Van Stryland, E.W. (1990) Sensitive Measurement of Optical Nonlinearities Using a Single Beam. *IEEE Journal of Quantum Electronics*, **26**, 760-769.

http://dx.doi.org/10.1109/3.53394

[24] Demirbas, U., Sennaroglu, A. and Somer, M. (2006) Synthesis and Characterization of Diffusion-Doped Cr^{2+}:ZnSe and Fe^{2+}:ZnSe. *Optical Materials*, **28**, 231-240. http://dx.doi.org/10.1016/j.optmat.2004.10.022

[25] Il'ichev, N.N., Shapkin, P.V., Gulyamova, E.S., Kulevsky, L.A. and Nasibov, A.S. (2010) Diffusion Coefficient of Fe^{2+} in Single-Crystal ZnSe. *Inorganic Materials*, **46**, 112-115. http://dx.doi.org/10.1134/S0020168510020044

[26] Avizonis, P.V. and Grotbeck, R.L. (1966) Experimental and Theoretical Ruby Laser Amplifier Dynamics. *Journal of Applied Physics*, **37**, 687-693. http://dx.doi.org/10.1063/1.1708238

[27] Kir'yanov, A.V. and Il'ichev, N.N. (2005) Nonlinear Resonant Change in Refractive Index of a Doped Saturable Medium at Short-Pulse Excitation. *Laser Physics Letters*, **2**, 485-488. http://dx.doi.org/10.1002/lapl.200510029

[28] Il'ichev, N.N., Kir'yanov, A.V., Shapkin, V.P., Nasibov, S.A. and Mosaleva, S.Ye. (2005) Nonlinear Change in Refractive Index of Co^{2+}:ZnSe at Short-Pulse Single-Beam 1.54-μm Z-Scan Probing. *Applied Physics B*, **81**, 83-91. http://dx.doi.org/10.1007/s00340-005-1860-z

[29] Muller, O., Lutz, Y., Teissier, A., Moeglin, J.P. and Keller, V. (2010) Optical Limiting Behavior of Carbon Nanotubes Exposed to Infrared Laser Irradiations Studied by the Z-Scan Technique. *Applied Optics*, **49**, 1097-1103. http://dx.doi.org/10.1364/AO.49.001097

[30] Xie, R., Li, L., Li, Y., Liu, L., Xiao, D. and Zhu, J. (2011) Fe:ZnSe Semiconductor Nanocrystals: Synthesis, Surface Capping, and Optical Properties. *Journal of Alloys and Compounds*, **509**, 3314-3318. http://dx.doi.org/10.1016/j.jallcom.2010.12.046

[31] Surma, M., Godlewski, M. and Surkova, T.P. (1994) Iron and Chromium Impurities as Centers of Nonradiative Recombination. *Physical Review B*, **50**, 8319-8324. http://dx.doi.org/10.1103/PhysRevB.50.8319

[32] Surkova, T.P., Kaczor, P., Zakrewski, A.J., Swiatek, K., Ivanov, V.Yu., Godlewski, M., Polimeni, A., Eaves, L. and Giriat, W. (2000) Optical Properties of ZnSe, ZnCdSe and ZnSSe Alloys Doped with Iron. *Journal of Crystal Growth*, **214-215**, 576-580. http://dx.doi.org/10.1016/S0022-0248(00)00156-1

[33] Il'ichev, N.N., Pashinin, P.P., Gulyamova, E.S., Bufetova, G.A., Shapkin, P.V. and Nasibov, A.S. (2014) Linear and Nonlinear Transmission of Fe^{2+}-Doped ZnSe Crystals at a Wavelength of 2940 nm in the Temperature Range 20-220˚C. *Quantum Electronics*, **44**, 213-216. http://dx.doi.org/10.1070/QE2014v044n03ABEH015323

[34] Mirov, S.B., Fedorov, V.V., Moskalev, I.S. and Martyshkin, D.V. (2007) Recent Progress in Transition-Metal-Doped II-VI Mid-IR Lasers. *IEEE Journal of Selected Topics in Quantum Electronics*, **13**, 810-822. http://dx.doi.org/10.1109/JSTQE.2007.896634

[35] Mirov, S.B., Fedorov, V.V., Martyshkin, D.V., Moskalev, I.S., Mirov, M.S. and Gapontsev, V.P. (2011) Progress in Mid-IR Cr^{2+} and Fe^{2+} Doped II-VI Materials and Lasers (Invited). *Optical Materials Express*, **1**, 898-910. http://dx.doi.org/10.1364/OME.1.000898

[36] Velikanov, S.D., Danilov, V.P., Zakharov, N.G., Il'ichev, N.N., Kazantsev, S.Yu., Kalinushkin, V.P., Kononov, I.G., Nasibov, A.S., Studenikin, M.I., Pashinin, P.P., Firsov, K.N., Shapkin, P.V. and Shchurov, V.V. (2014) Fe^{2+}:ZnSe Laser Pumped by a Nonchain Electric-Discharge HF Laser at Room Temperature. *Quantum Electronics*, **44**, 141-144. http://dx.doi.org/10.1070/QE2014v044n02ABEH015341


Advances in
Bioscience and Biotechnology


American Journal of
Analytical Chemistry


American Journal of
Plant Sciences
Special Issue on Photosynthesis

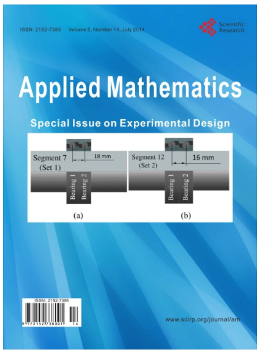
Applied Mathematics
Special Issue on Experimental Design

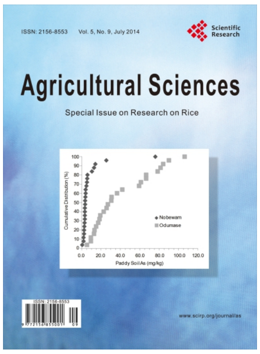
Agricultural Sciences
Special Issue on Research on Rice

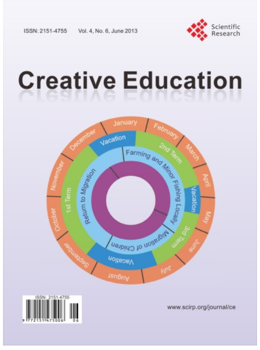
Creative Education

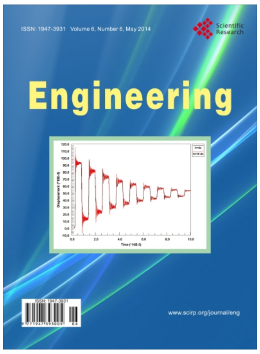
Engineering


Food and Nutrition Sciences

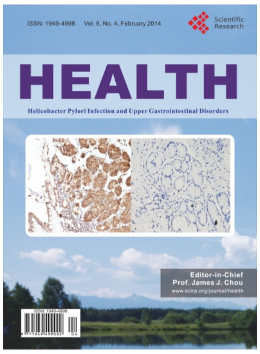
HEALTH
Helicobacter Pylori Infection and Upper Gastrointestinal Disorders
Editor-in-Chief
Prof. James J. Chou


Journal of Computer
and Communications


Journal of Cancer Therapy
Special Issue on Bone Tumor Research

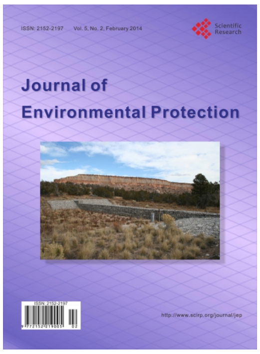
Journal of
Environmental Protection

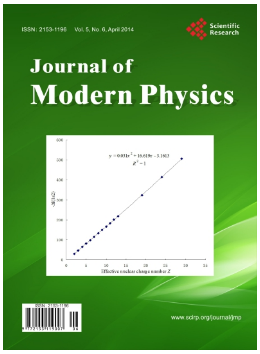
Journal of
Modern Physics


Modern Economy

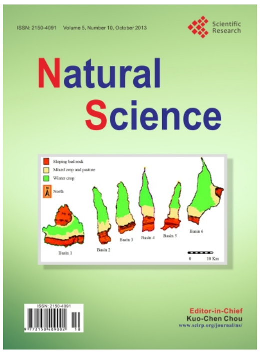
Natural
Science
Editor-in-Chief
Kuo-Chen Chou

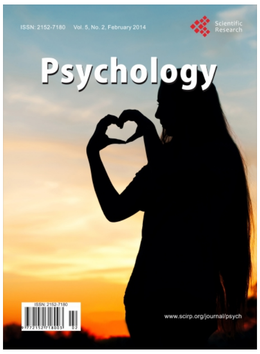
Psychology